Bima Journal of Science and Technology, Vol. 9(1B) Apr, 2025 ISSN: 2536-6041

DOI: 10.56892/bima.v9i1B.1280

Modeling and Optimization of Fresh Properties of Kenaf Biofibrous Concrete Using Response Surface Methodology

Ogunbode Ezekiel Babatunde[1]*, Moses Daniel Walbe[2], Adamu Bala[3]., Mohoro Ibrahim Sarki[4] and Lawal Temitope Adesina[5]

[1]Department of Building, Federal University of Technology, Minna, Niger State, Nigeria
[2]Department of Building Technology, Federal Polytechnic Bida, Níger State, Nigeria
[3,4]Department of Building Technology, Níger State Poytechnic, Zungeru, Níger State, Nigeria
[5]Department of Building, Ladoke Akintola University of Technology, Ogbomoso, Oyo State, Nigeria

Corresponding Author: ezekiel@futminna.edu.ng

ABSTRACT

The pursuit of sustainable construction materials has led to growing interest in biofibrous concrete reinforced with natural fibres. This study investigates the influence of kenaf fibre length and volume fraction on the fresh properties of concrete—slump, compacting factor, and Vebe time—using Response Surface Methodology (RSM). A face-centred Central Composite Design (CCD) was employed to model and optimize the mix design. Experimental results revealed that, increasing fibre length and content significantly reduced workability, with slump decreasing from 90 mm to 5 mm as fibre volume increased from 0.5% to 1.5% and length from 25 mm to 75 mm. Regression models demonstrated strong predictive accuracy ($R^2 > 90\%$) across all responses. Multi-response optimization using desirability function identified the ideal mix as 36.87 mm fibre length and 0.78% volume fraction, yielding a predicted slump of 49.99 mm, compacting factor of 0.90, and Vebe time of 18.23s. Laboratory validation produced close agreement, with prediction errors below 8%. These findings affirm the potential of kenaf fibres in sustainable concrete applications and align with earlier findings on natural fibre concrete systems, reinforcing the robustness of RSM in mix design optimization.

Keywords: biofibrous concrete, Central Composite Design (CCD), fresh concrete properties, kenaf fibre, optimization, Response Surface Methodology (RSM),

INTRODUCTION

Sustainable construction practices have increasingly prioritized the integration of renewable materials in concrete composites to reduce environmental impact and reliance on synthetic fibres. Among natural alternatives, kenaf fibre (*Hibiscus cannabinus* L.) has garnered considerable attention due to its high tensile strength, biodegradability, and local availability in tropical regions such as Africa and Southeast Asia (Ramesh, 2016; Huang *et al*., 2025). The inclusion of natural fibres in concrete offers dual benefits—environmental sustainability and enhanced post-cracking behaviour. However, the incorporation of such fibres can compromise fresh concrete properties, particularly workability and consistency, due to their high surface area, tendency to clump, and water absorption characteristics (Hamada *et al.,* 2023). Key influencing parameters include fibre length and volume fraction, which must be carefully controlled to achieve optimal performance.

Response Surface Methodology (RSM) offers a powerful statistical tool for evaluating and optimizing the effects of multiple input variables on desired responses through minimal experimentation (Montgomery, 2017). Although RSM has been extensively applied to conventional and fibre-reinforced concrete systems, its application to Kenaf Fibre Reinforced

Concrete (KFRC) particularly for fresh-state behaviour remains limited in scope and depth. This study addresses this gap by developing and validating RSM-based models for predicting and optimizing the fresh properties (slump, compacting factor, and Vebe time) of kenaf biofibrous concrete using a face-centred Central Composite Design. The results provide a robust framework for sustainable mix design and reinforce the viability of kenaf fibres in green construction applications.

MATERIALS AND METHODS

Experimental Design

A face-centered Central Composite Design (CCD) was used within the RSM framework to examine the effects of two independent variables: fibre length (X_1) and fibre volume fraction (X_2). Each variable was studied at three levels, producing 11 experimental runs, including five center-point replications to estimate curvature and error. The responses measured were slump (mm), compacting factor, and Vebe time (s). The experimental matrix is presented in Table 1.

Table 1: Design of Experiments (DOE) Using CCD.

Run	Fibre Length (mm)	Fibre Volume Fraction (%)
1	50	1.0
2	50	1.0
3	25	0.5
4	75	1.0
5	50	1.0
6	25	1.5
7	50	1.5
8	75	1.5
9	25	1.0
10	50	0.5
11	75	0.5

Mix Proportioning

The concrete mixture was designed to achieve a target compressive strength of 30 MPa. A constant water-to-cement ratio of 0.45 and a sand-to-total aggregate ratio of 0.72 were maintained across all mixes. Fibre content was varied per the design matrix, and additional water was added to account for the absorption capacity of the fibres.

Test Methods

Fresh concrete properties were assessed according to standardized procedures. The slump test was conducted following ASTM C143/C143M (2020) to evaluate workability. The compacting factor test was carried out per BS 1881-103 (1993) to measure the degree of internal compaction. The Vebe time test, performed in accordance with BS EN 12350-3 (2019), evaluated consistency and stiffening behaviour under vibration. All tests were performed immediately after mixing to ensure the accuracy of fresh-state measurements. The operational setups for the slump, compacting factor, and Vebe time tests are illustrated in Figures 1, 2, and 3, respectively.

Statistical Analysis

Data analysis was conducted using Minitab 21 software. Response Surface Methodology (RSM) was employed to develop second-order regression models for each response. Model adequacy was assessed through Analysis of Variance (ANOVA), significance testing (p-values < 0.05), and goodness-of-fit indicators including the coefficient of determination (R^2) and adjusted R^2. Diagnostic plots such as normal probability, residuals versus fits, and Pareto charts were used to verify assumptions of normality, constant variance, and independence of residuals, ensuring the reliability and robustness of the regression models.

DOI: 10.56892/bima.v9i1B.1280

(a) (b) (c)

Figure 1: An Operational Procedure for Slump Test: (a) Abram's Slump Apparatus, (b and c) Measurement of Slump

(a) Set up for Vebe test (b) VB apparatus in operation

Figure 2: Operational Procedures for Vebe Test

DOI: 10.56892/bima.v9i1B.1280

(a) (b) (c) (d)

(a) set up for compacting factor (b) filling concrete into the pan (c) measurement of Slump (d) vibrating table

Figure 3: Operational Procedures for Compacting Factor Test

RESULTS AND DISCUSSION

Influence of Fibre Parameters on Fresh Concrete Properties

The experimental results (Table 2) show a clear relationship between kenaf fibre parameters and the fresh properties of concrete. As fibre length and volume fraction increased, all three measured responses, slump, compacting factor, and Vebe time deteriorated progressively. This trend highlights the sensitivity of fresh concrete workability to the geometry and dosage of added fibres. Notably, the mix containing 25 mm fibres at 0.5% volume fraction achieved a slump of 90 mm and compacting factor of 0.923, indicating excellent flow and ease of placement. In contrast, at the upper boundary condition (75 mm length, 1.5% volume), the slump dropped drastically to 5 mm, and the compacting factor declined to 0.782. These values signify that, beyond a certain threshold, fibre entanglement and absorption critically impair workability, a behaviour also reported by (Ogunbode *et al*., 2022). Figures 4 and 5 illustrate the contour and surface plot of slump versus fibre parameters. The nonlinear response surface confirms significant interaction effects. From a practical perspective, a slump of 54 mm, obtained under optimized conditions can be classified as medium workability per EN 206, making it suitable for conventional vibrated concreting methods such as beams and slabs. For highly congested reinforcement or pump applications, lower fibre doses would be recommended to achieve higher flow. This highlights the importance of balancing eco-fibre benefits with construction practicality.

In addition to slump, contour and surface plots were developed for compacting factor and Vebe time to evaluate how fibre parameters influence these responses. Figures 6 and 7 show that, compacting factor decreases with increasing fibre length and volume fraction. The steepest drop occurs at high volume fractions (1.5%) and longer fibre lengths (75 mm), confirming that excessive fibre content hampers internal particle rearrangement during compaction.

Bima Journal of Science and Technology, Vol. 9(1B) Apr, 2025 ISSN: 2536-6041

DOI: 10.56892/bima.v9i1B.1280

Conversely, higher compacting factor values (>0.90) were recorded at the lower end of both parameters, which reflects more workable mixes suitable for conventional consolidation. Figures 8 and 9 illustrate the effect of fibre parameters on Vebe time, which increases sharply with longer fibres and higher volume content. Vebe times over 50 seconds were observed in mixes with 75 mm fibres at 1.5% volume, signifying stiff mixes that require significant vibration to achieve compaction. On the other hand, mixes with short fibres and low volume fractions exhibited Vebe times below 10 seconds, ideal for flowable concrete.

The 3D surfaces and contours for both compacting factor and Vebe time demonstrate strong interaction effects and non-linearity, confirming the necessity of second-order models and validating the effectiveness of RSM for process optimization.

Table 2: Experimental Results of Fresh Properties

Run	Fibre Length (mm)	Fibre Volume Fraction (%)	Slump (mm)	Compacting Factor	VeBe Time Consistometre (s)
1	50	1.0	25	0.867	33
2	50	1.0	25	0.867	33
3	25	0.5	90	0.923	4
4	75	1.0	10	0.787	43
5	50	1.0	25	0.867	33
6	25	1.5	25	0.812	40
7	50	1.5	10	0.829	52
8	75	1.5	5	0.782	61
9	25	1.0	40	0.898	16
10	50	0.5	70	0.911	12
11	75	0.5	40	0.864	18

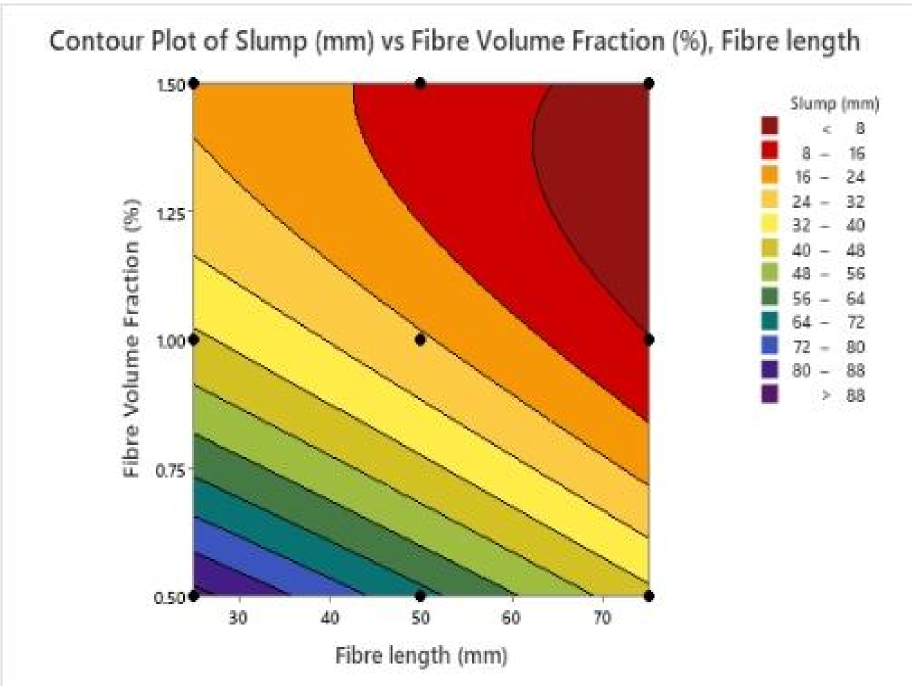

Figure 4: Contour Plot Showing the Effect of Fibre Length and Fibre Volume Fraction on Slump.

Bima Journal of Science and Technology, Vol. 9(1B) Apr, 2025 ISSN: 2536-6041
DOI: 10.56892/bima.v9i1B.1280

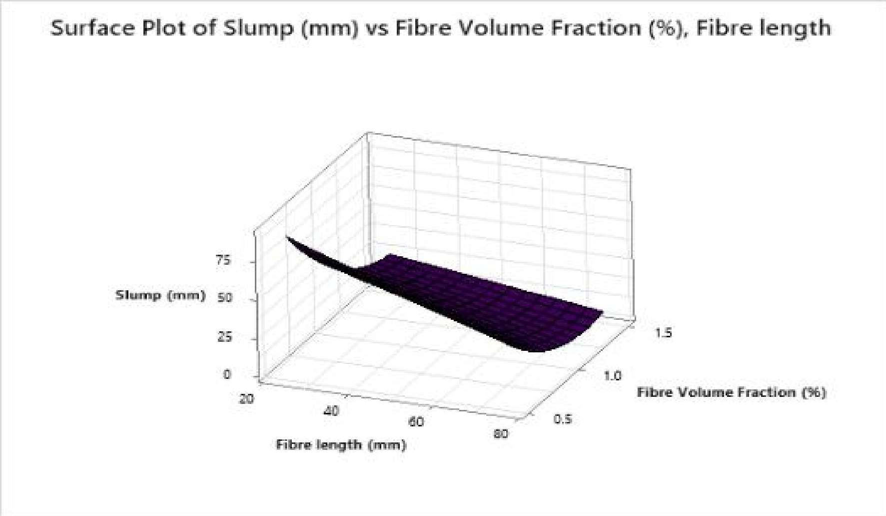

Figure 5: 3D Surface Plot Illustrating the Interaction Effects of Fibre Parameters on Slump.

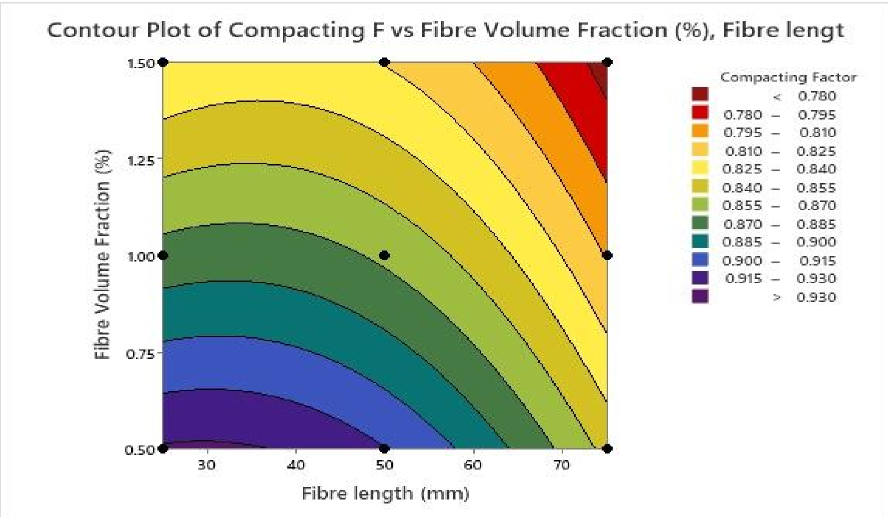

Figure 6: Contour Plot of Compacting Factor as a Function of Fibre Length and Volume Fraction.

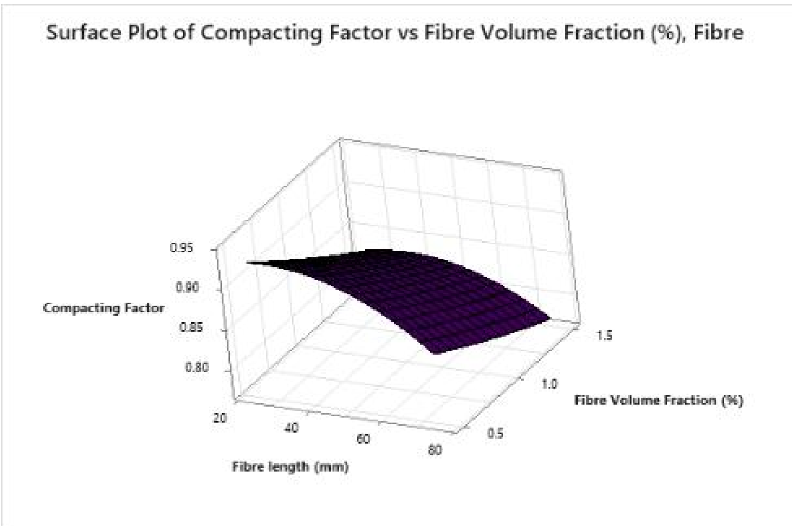

Figure 7: 3D Surface Plot Showing the Effect of Fibre Parameters on Compacting Factor.

DOI: 10.56892/bima.v9i1B.1280

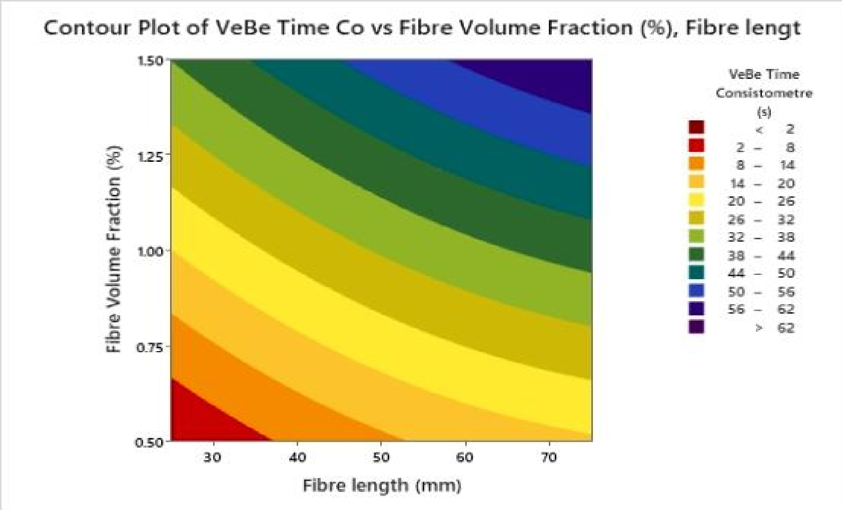

Figure 8: Contour Plot of Vebe Time with Respect to Fibre Length and Volume Fraction.

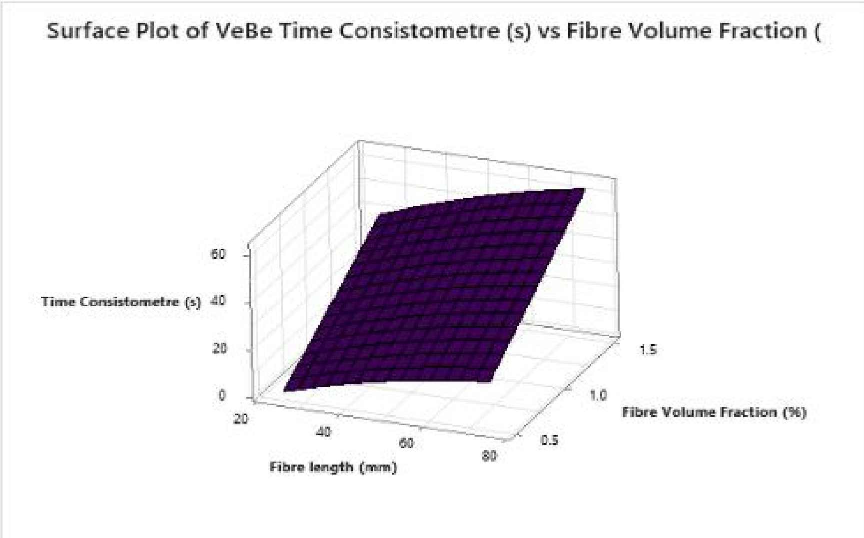

Figure 9: 3D Surface Plot Illustrating how Fibre Length and Volume Influence Vebe Time

Regression Modeling and ANOVA

Quadratic models were developed for all responses. For slump, the model exhibited $R^2 = 99.39\%$, indicating excellent prediction. Similar results were achieved for compacting factor ($R^2 = 93.17\%$) and Vebe time ($R^2 = 98.91\%$). ANOVA revealed that, both fibre length and volume fraction were statistically significant ($p < 0.05$), with interaction effects contributing modestly.

The second-order polynomial model developed for slump is shown in Equation (1).

$$Slump=201.7-1.267X_1-203.3X_2-0.00000X_1^2+60.00X_2^2+0.600X_1X_2 \quad (1)$$

(where X_1 = Fibre Length, X_2 = Fibre Volume Fraction)

The second-order polynomial model developed for compacting factor is presented in Equation (2), while the second-order polynomial model developed for vebe time is illustrated in Equation (3) respectively.

DOI: 10.56892/bima.v9i1B.1280

$$\text{Compacting Factor}=0.9673+0.00203X_1-0.1436X_2-0.000039X_1^2+0.0115X_2^2+0.000580X_1X_2 \quad (2)$$

$$\text{VeBe Time}=-29.33+0.644X_1+1.2X_2-0.00371X_1^2+0.74X_2^2+0.140X_1X_2 \quad (3)$$

(where X_1 = Fibre Length, X_2 = Fibre Volume Fraction)

To assess model adequacy, a series of diagnostic plots were generated for all three responses (slump, compacting factor, and Vebe time). The normal probability plots (Figures 10, 11, and 12) show that, residuals align closely with the reference line, confirming that the error terms follow a normal distribution. The model exhibited strong statistical performance with an R^2 value of 99.39%, 93.17% and 98.91% for slump, compacting factor and vebe time respectively, indicating that the model accounts for a substantial proportion of the variability in the response.

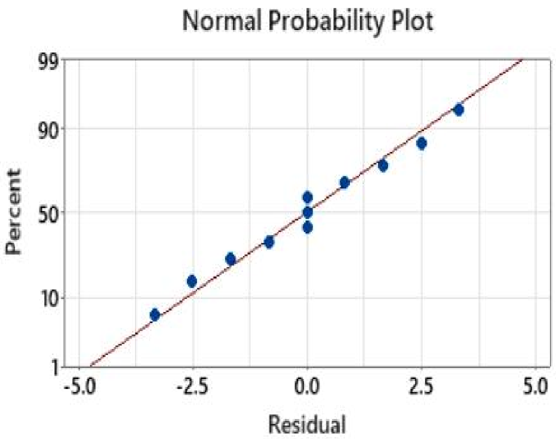

Figure 10: Normal Probability Plot of Residuals for Slump Model.

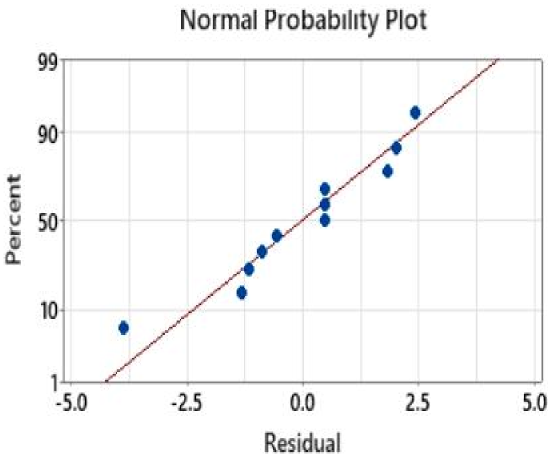

Figure 11: Normal Probability Plot of Residuals for Compacting Factor Model.

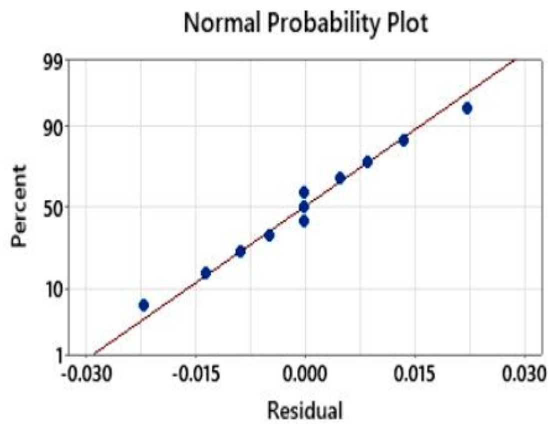

Figure 12: Normal Probability Plot of Residuals for Vebe Time Model.

The Pareto charts of standardized effects (Figures 13, 14, and 15) highlight the statistical significance of main effects and interactions, with fibre volume fraction consistently emerging as the most influential factor across responses. The Pareto charts further confirms that both fibre length and fibre volume fraction significantly influence slump, compacting factor and Vebe time, with the volume fraction being the more dominant factor. These observations agree with results from (Zhao *et al.,*2022 & Xiong *et al.,*2022), who reported that, higher fibre content restricts internal movement of concrete particles, leading to longer vibration times during consistency testing. Also, the study of Amiandamhen *et al.*, (2016) and Ogunbode *et al.,* (2022), corroborated the findings that increasing fibre content tends to hinder compaction due to inter-fibre interaction and balling effects. The interaction between fibre length and volume, although less significant statistically, contributed to slight non-linear behaviour in the data.

Bima Journal of Science and Technology, Vol. 9(1B) Apr, 2025 ISSN: 2536-6041
DOI: 10.56892/bima.v9i1B.1280

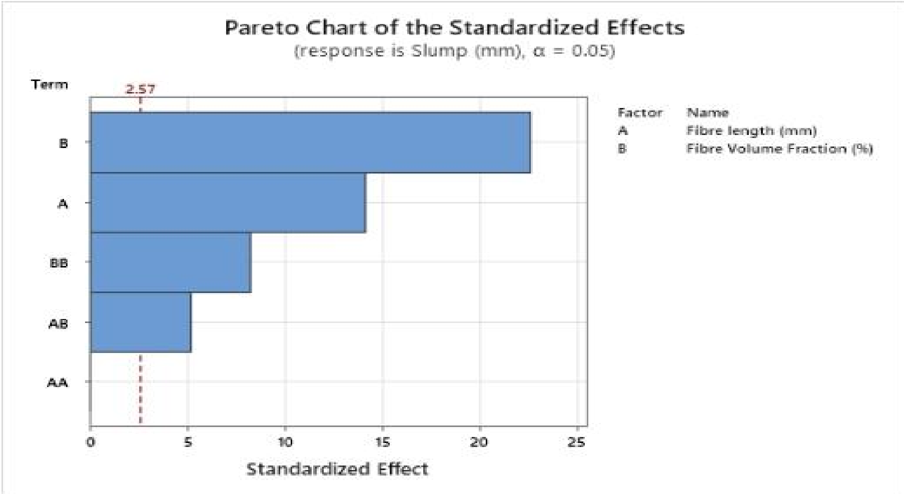

Figure 13: Pareto Chart of Standardized Effects for Slump Model.

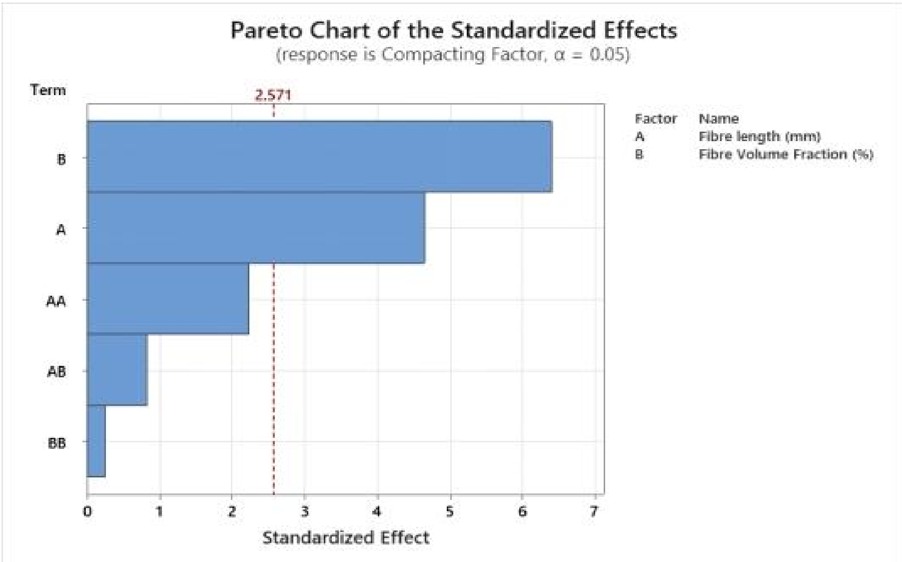

Figure 14. Pareto Chart of Standardized Effects for Compacting Factor Model.

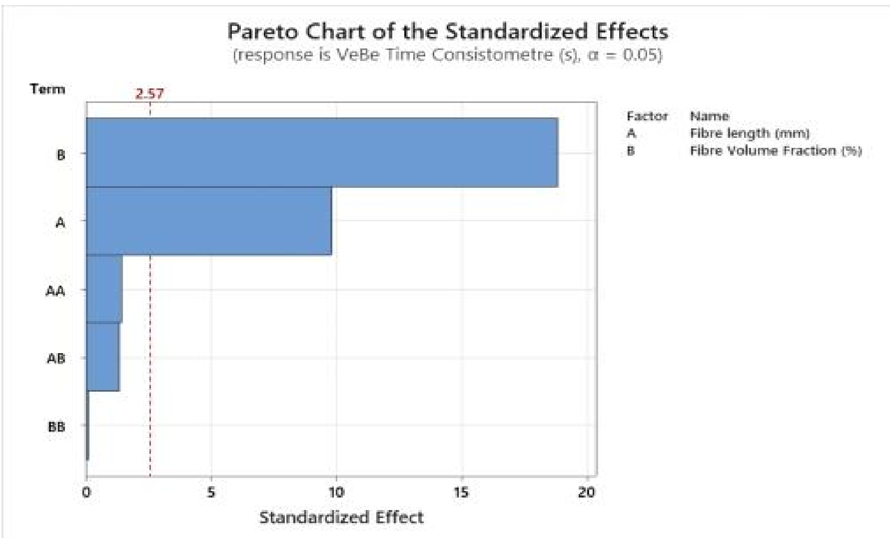

Figure 15: Pareto Chart of Standardized Effects for Vebe Time Model.

Bima Journal of Science and Technology, Vol. 9(1B) Apr, 2025 ISSN: 2536-6041

DOI: 10.56892/bima.v9i1B.1280

The residuals versus fitted values plots (Figures 16, 17, and 18) demonstrate a random scatter of residuals around the horizontal axis, indicating homoscedasticity and absence of systematic error. Across all models, no outliers or leverage points were detected, and residual distributions were approximately symmetrical. These diagnostics confirm that the underlying assumptions of regression normality, independence, and constant variance of residuals were satisfactorily met, thereby validating the use of second-order polynomial models in this study. The absence of curvature or funnel-shaped distribution reinforces the model's adequacy for prediction purposes. Therefore, diagnostic assessment confirms the statistical soundness of the Vebe time regression model, making it suitable for optimization and practical decision-making in eco-concrete design.

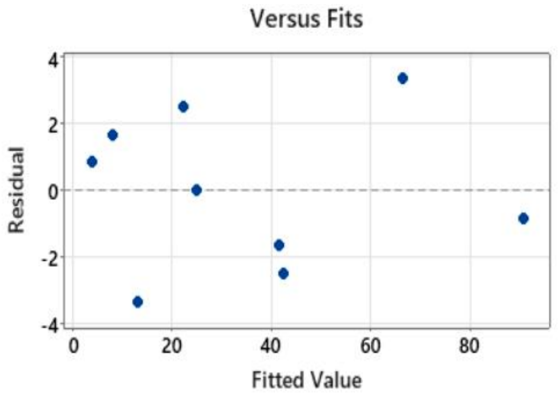

Figure 16: Residual Versus Fitted Values Plot for Slump Model.

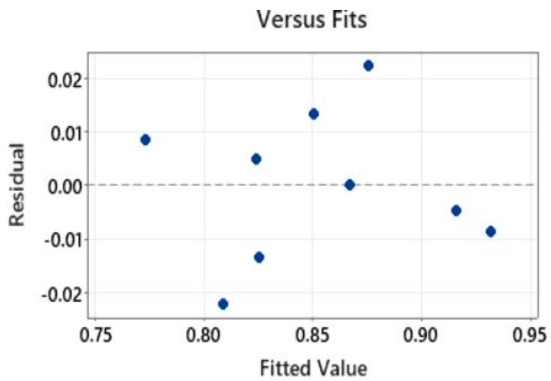

Figure 17. Residual Versus Fitted Values Plot for Compacting Factor Model.

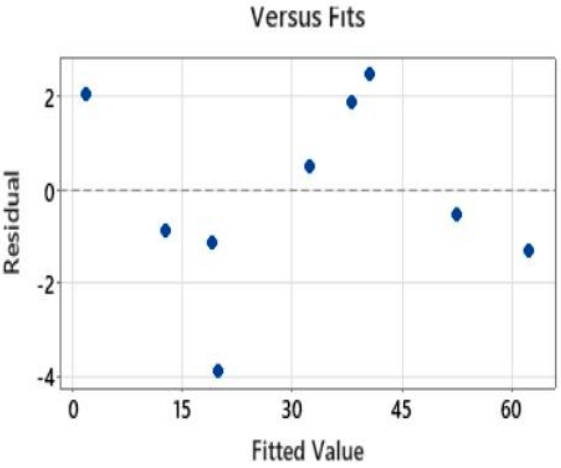

Figure 18: Residual Versus Fitted Values Plot for Vebe Time Model.

Optimization Using Desirability Function

Response Surface Methodology was employed to optimize the fresh concrete properties by simultaneously maximizing slump and compacting factor while minimizing Vebe time. A multi-response desirability function approach was applied using Minitab 21 software to identify the optimal combination of fibre parameters. The optimal mix was achieved at a fibre length of 36.87 mm and fibre volume fraction of 0.78%, yielding the following predicted responses: (1) Slump: 49.99 mm, (2) Compacting Factor: 0.900 (3) Vebe Time: 18.23 seconds. This solution returned a composite desirability score of 0.909 (Table 3), indicating a highly favourable balance between the competing objectives. The identified mix falls within a medium workability range suitable for typical on-site casting applications, offering adequate flow without segregation or the need for excessive vibration. This optimization demonstrates that with precise tuning of fibre geometry and content, Kenaf Biofibrous Concrete (KBFC) can meet the practical workability requirements while maintaining its environmental benefits. The approach also validates the effectiveness of RSM as a predictive and decision-support tool for sustainable material formulation.

Bima Journal of Science and Technology, Vol. 9(1B) Apr, 2025 ISSN: 2536-6041

DOI: 10.56892/bima.v9i1B.1280

Table 3: Optimized Values Using RSM

Parameter	Value
Fibre Length (mm)	36.87
Fibre Volume (%)	0.78
Predicted Slump (mm)	49.99
Compacting Factor	0.900
Vebe Time (s)	18.23
Composite Desirability	0.909

Experimental Validation

Validation experiments confirmed the model's accuracy. The actual results showed a slump of 54 mm, compacting factor of 0.95, and Vebe time of 19 s. All measured values were within 8% of model predictions (Table 4), verifying the robustness of the developed regression models. Figure 19 shows a strong agreement between predicted and actual responses across all parameters. These results support the reliability of RSM in capturing nonlinear effects in fibre-reinforced systems. While this study focused specifically on kenaf fibres, the modelling approach, particularly the use of a face-centered CCD can be extended to other natural fibres such as jute, hemp, bamboo, or coir, with appropriate calibration. Such generalizability reinforces the utility of RSM as a versatile tool for optimizing bio-based concrete compositions in line with green construction goals.

Table 4: Model Validation Results

Response	Predicted	Actual	Difference	% Error
Slump (mm)	49.99	54	+4.01	7.43%
Compacting Factor	0.900	0.950	+0.050	5.26%
Vebe Time (s)	18.23	19	+0.77	4.05%

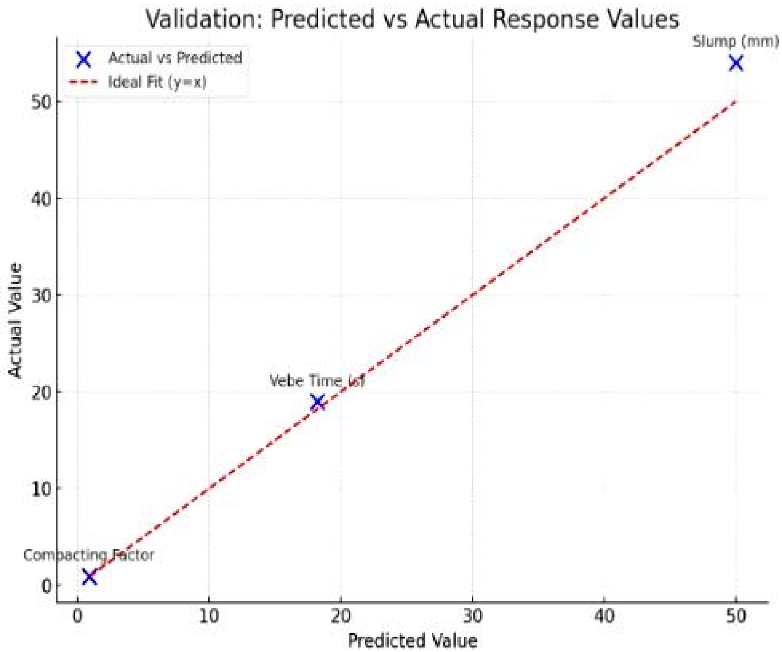

Figure 19: Predicted Versus Actual Response Values for Slump, Compacting Factor, and Vebe Time.

Each point shows how close model predictions were to the lab-measured results. The red dashed line represents a perfect match (ideal prediction) which confirms excellent prediction accuracy.

CONCLUSION

This study successfully modeled and optimized the fresh properties of kenaf biofibrous concrete using Response Surface

DOI: 10.56892/bima.v9i1B.1280

Methodology with a face-centered Central Composite Design (CCD). Fibre length and volume fraction were identified as significant factors influencing slump, compacting factor, and Vebe time. The optimal combination 36.87 mm fibre length and 0.78% volume fraction was shown to produce concrete with medium workability and consistent internal compaction, aligning well with real-world constructability requirements. Importantly, this represents the first reported study to model and optimize kenaf fibre reinforced concrete using a face-centered CCD and desirability-based multi-response optimization. The regression models demonstrated high predictive accuracy and were validated experimentally with errors under 8%, confirming their applicability in practice. From a construction standpoint, the optimized mix design is not only suitable for field applications such as slabs, beams, and general structural concrete, but also adaptable to standard production and placement methods without extensive modifications. Given the growing emphasis on sustainable and low-carbon materials, this approach offers a scalable, eco-friendly solution that can inform future guidelines or inclusion in concrete design codes related to natural fibre additives. Future research should investigate the mechanical, durability, and long-term performance characteristics of these optimized mixes, potentially expanding their use in reinforced structural elements and high-performance green concrete applications.

REFERENCES

Amiandamhen, S. O., Izekor, D. N., & Balogun, A. O. (2016). Performance Characteristics of Treated Kenaf Bast Fibre Reinforced Cement Composite. *Journal of the Indian Academy of Wood Science*, *13(2)*, 156-160.

ASTM C143/C143, (2020). *Standard Test Method for Slump of Hydraulic-Cement Concrete*. ASTM International. https://www.astm.org/c0143_c0143m-20.html

BS 1881-103, (1993). *Testing Concrete. Method for Determination of Compacting Factor*. British Standards Institution, London.

BS EN 12350-3, (2019). *Testing Fresh Concrete. Vebe Test*. British Standards Institution, London.

BS EN 12620, (2013) *Aggregates for Concrete*. British Standards Institution, London.

BS EN 206, (2013). Concrete – Specification, Performance, Production and Conformity. British Standards Institution, London.

Hamada, H. M., Shi, J., Al Jawahery, M. S., Majdi, A., Yousif, S. T., & Kaplan, G. (2023). Application of Natural Fibres in Cement Concrete: A Critical Review. *Materials Today Communications*, *35*, 105-833. https://doi.org/10.1016/j.mtcomm.2023.105833

Huang, Y., Sultan, M. T. H., Shahar, F. S., Łukaszewicz, A., Oksiuta, Z., & Grzejda, R. (2025). Kenaf Fiber-Reinforced Biocomposites for Marine Applications: A Review. *Materials*, *18*(5), 999.

Montgomery, D. C. (2017). *Design and Analysis of Experiments* (9th ed.). John Wiley & Sons.

Ogunbode, E. B., Garba, Y. Y., Musa, B., Oliver, M., Daniya, N. S., & Ekekezie, C. U. (2022). Effects of Kenaf Fibre on Fresh Properties of Fibrous Concrete. *Environmental Technology and Science Journal, 13(1),* 31–40.

Ramesh, M. (2016). Kenaf (Hibiscus Cannabinus L.) Fibre Based Bio-Materials: A Review on Processing and Properties. *Progress in Materials Science*, *78*, 1-92. https://doi.org/10.1016/j.pmatsci.2015.10.001

Xiong, G., Wang, C., Zhou, S., & Zheng, Y. (2022). Study on Dispersion Uniformity and Performance Improvement ofSteel Fibre Reinforced Lightweight Aggregate Concrete by Vibrational Mixing. *Case Studies in Construction Materials*, *16*, 1093.

Zhao, M., Li, J., & Xie, Y. M. (2022). Effect of Vibration Time on Steel Fibre Distribution and Flexural Behaviours of Steel Fibre Reinforced Concrete with Different Flowability. *Case Studies in Construction Materials*, *16*, 11-14.